

Spin Symmetry of the Bilayer Graphene Groundstate

Frank Freitag, Markus Weiss,* Romain Maurand,

Jelena Trbovic, and Christian Schönenberger

Department of Physics, University of Basel,

Klingelbergstrasse 56, CH-4056 Basel, Switzerland

(Dated: November 8, 2018)

Abstract

We show nonlinear transport experiments on clean, suspended bilayer graphene that reveal a gap in the density of states. Looking at the evolution of the gap in magnetic fields of different orientation, we find that the groundstate is a spin-ordered phase. Of the three possible gapped groundstates that are predicted by theory for equal charge distribution between the layers, we can therefore exclude the quantum anomalous Hall phase, leaving the layer antiferromagnet and the quantum spin Hall phase as the only possible gapped groundstates for bilayer graphene.

PACS numbers: 72.80 Vp, 73.22 Gk, 73.22 Pr, 73.23.-b, 73.43 Qt

*Electronic address: Markus.Weiss@unibas.ch

The isolation of monolayer graphene [1] has given a new twist to the research on two-dimensional electron systems, because graphene as a zero-gap semiconductor with a pseudo-relativistic dispersion relation shows fundamentally new effects such as Klein-tunneling [2] that do not occur in conventional two-dimensional electron gases (2DEGs) with a finite bandgap and a parabolic dispersion. The presence of two atoms in the graphene unit cell is described by a sublattice-pseudospin, which acquires a Berry phase of π on closed k-space trajectories that include one of the K-points, which are the corner points of the first Brillouin zone and also constitute the Fermi surface of charge neutral graphene. One consequence of this Berry phase is an unusual Landau level spectrum that leads to the occurrence of quantum Hall plateaus at conductances of half integer multiples of the Landau level degeneracy [3, 4]. As the pseudospin degree of freedom is present also in Bernal stacked graphene multilayers, they can be described by one low energy theory that explicitly includes the chiral nature of the charge carriers [5].

Bilayer graphene in A-B stacking is a 2DEG with a parabolic dispersion for small energies $|E| \ll \gamma_1$, where $\gamma_1 \approx 0.4$ eV is the interlayer hopping parameter that links two atoms sitting on top of each other [6]. As a consequence of the parabolic dispersion there is a finite density of states at the charge neutrality point (CNP) which, together with the weak dispersion leads to strong electron-electron interactions that make bilayer graphene at the CNP unstable towards interaction induced symmetry breaking [7–13].

The exact nature of the electronic groundstate of bilayer graphene at charge neutrality is being discussed intensely at the moment, with numerous theoretical investigations suggesting a large number of phases. In each of these phases some of the three discrete degrees of freedom in bilayer graphene (spin, valley and layer) undergo a transition to a lower symmetry state. While it is clear that for large magnetic fields quantum Hall ferromagnetism will occur [14], and that for strong perpendicular electric fields a layer polarized state will form [7, 15], the nature of the groundstate at $B=0$ and $E_\perp=0$ is less obvious. Whereas some experiments have found a conductive groundstate [16, 17], the majority of experimental results [17–24] point to an insulating groundstate, an observation that limits the number of possible phases to the ones that are bulk gapped.

In this communication we show experimental results that further elucidate the nature of the bilayer graphene groundstate. We have performed nonlinear conductance measurements at the CNP of clean, suspended bilayer graphene samples as a function of magnetic fields

oriented perpendicular and parallel to the graphene layer. Our measurements show a gap, that increases strongly only in a perpendicular magnetic field, whereas it stays constant to a high precision in a magnetic field that is exactly parallel to the bilayer plane. Our results allow us to make a statement about the spin order of the bilayer graphene groundstate and therefore to narrow down further the number of possible candidates for the electronic groundstate of bilayer graphene.

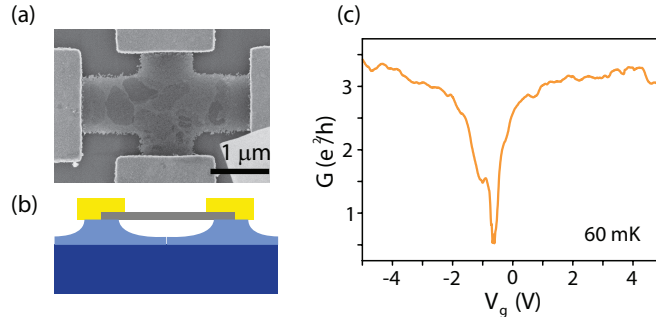


FIG. 1: a) SEM micrograph of the sample. b) Schematic of the sample structure. c) Conductance G as a function of backgate voltage V_g .

Bilayer graphene was exfoliated from natural graphite onto oxidized silicon wafers, and contacted with Cr/Au electrodes using e-beam lithography. The bilayer was suspended by partly removing the oxide in a buffered hydrofluoric acid wet etch and subsequent critical point drying, as described in [22]. The data shown here were obtained on a four-terminal sample in Hall-cross geometry that had been shaped by an Ar/O₂ plasma dry etching process (figure 1). We measured two-terminal conductance on contacts on opposite sides of the Hall-cross with the other two terminals floating or connected to a high-impedance voltmeter for Hall measurements. All measurements were done in a dip-stick dilution refrigerator at base temperature ($T=60$ mK).

Figure 1 shows an SEM picture (a) and a schematic cross section (b) of the sample, together with backgate characteristics of the device (c) measured at $T=60$ mK after current annealing [22]. The charge neutrality point (CNP) is visible as a deep minimum in the conductance G measured as a function of gate voltage V_g at -0.6 V, indicating the formation of an insulating state around charge neutrality. The position of the CNP at a small negative gate voltage indicates a very small amount of residual dopants on the flake.

Figure 2a shows a measurement of the zero-bias conductance G as a function of gate

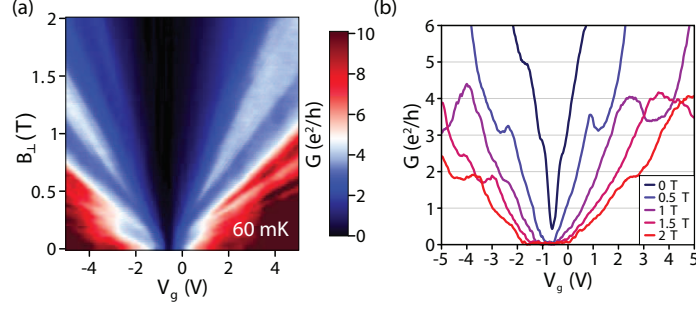


FIG. 2: a) Conductance G as a function of perpendicular magnetic field B_{\perp} and gate voltage V_g . b) Cuts through a) at several fixed magnetic fields.

voltage V_g and perpendicular magnetic field B_{\perp} . From the line cuts in figure 2b one can see that there is a quantum Hall state at filling factor $\nu=4$ developed for $B_{\perp} \geq 1.0\text{ T}$, giving a lower limit of $10\,000\text{ cm}^2/\text{Vs}$ for the charge carrier mobility. At higher fields additional intermediate plateaus start to occur, indicating a lifting of the spin and valley degeneracies.

Differential conductance $G_d=dI/dV$ at the CNP as a function of perpendicular magnetic field B_{\perp} and bias voltage V_{sd} is shown in figure 3a. Several line-cuts at different magnetic fields are shown in figure 3b. Similar to previous studies [20–22], we find a strong suppression of conductance around zero bias, together with a BCS-like overshoot at a finite voltage of $V_{sd} \approx 3.5\text{ mV}$, indicating the formation of an interaction induced broken symmetry state with a bulk gap.

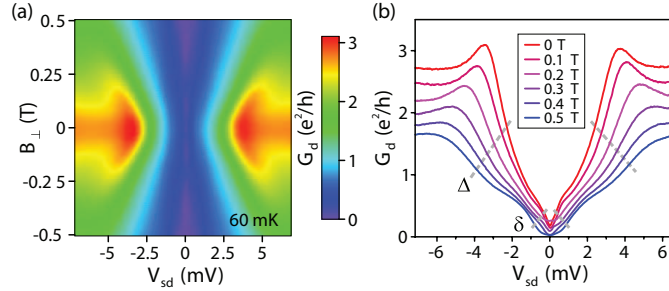


FIG. 3: a) Differential conductance G_d at the CNP as a function of perpendicular magnetic field B_{\perp} and bias voltage V_{sd} . b) Cuts through a) at several fixed magnetic fields.

The $G_d(V_{sd})$ curves in figure 3b show two inflection points that we associate with two different gap energy scales δ and Δ [21, 22]. Following the inflection points in finite perpendicular magnetic field, we find that the larger feature Δ increases linearly with 3.1 meV/tesla , whereas the smaller feature δ shows a weaker response of 1.7 meV/tesla , both of them how-

ever still much larger than the Zeeman energy for free electrons, which would amount to 0.116 meV/tesla [28]. As we have shown in previous studies [21, 22] the larger feature Δ only exists in a narrow range of gate voltage around the CNP, whereas the small feature δ persists over the whole gate range that is accessible with the present sample. We think that δ is due to localization in disordered areas on the sample perimeter, and that Δ has to be associated with an interaction induced broken symmetry state located in the center region of the sample.

Interaction effects in bilayer graphene have been described with the so-called broken symmetry state quasiparticle Hamiltonian

$$\mathcal{H} = - \left(\frac{p^2}{2m^*} \right) [\cos(2\phi_p) \sigma_x \pm \sin(2\phi_p) \sigma_y] - \vec{\Delta} \cdot \vec{\sigma} \quad (1)$$

with $\tan(\phi_p) = p_y/p_x$, m^* the effective mass, $\vec{\sigma}$ the layer pseudospin vector, + and - chosen for valley K and K', respectively, and $\vec{\Delta}$ the order parameter of the broken symmetry state [7, 9, 10, 20, 25]. For $\vec{\Delta} = (0, 0, \Delta_z)$ the groundstate is gapped and equation (1) predicts all electrons of the same spin and valley (the same spin-valley flavour) to be located in the same layer, a state that has also been described as a layer pseudospin magnet [7]. Eight qualitatively different groundstates with distinct distributions of the four spin-valley flavors across the two layers are possible. Three of them have no overall layer polarization, and can be assumed to be energetically favorable in case of vanishing external electric fields. These three states are the quantum anomalous Hall state (QAH)[11], the layer antiferromagnetic state (LAF), and the quantum spin Hall insulator (QSH). Their symmetries are determined by different order parameters in the quasiparticle Hamiltonian (1), namely $\Delta_z = \lambda \tau_z$ for the QAH, $\Delta_z = \lambda s_z$ for the LAF, and $\Delta_z = \lambda \tau_z s_z$ for the QSH. Here τ_z and s_z represent the valley pseudospin and the electron spin, respectively. Due to a peculiar k-space topology [25], each spin valley flavor has an intrinsic Hall conductivity, the direction of which is given by $\tau_z \cdot \text{sign}(\Delta_z)$: It depends on the valley and the sign of the order parameter in equation (1). While for the LAF and QSH states the (charge) Hall conductivities of the four different spin-valleys cancel out, in the QAH they add up, which means that for the QAH a nonzero quantized Hall conductance of $4e^2/h$ is expected even in the absence of an external magnetic field. Although no net charge Hall conductivity is expected for the QSH phase, the resulting edge states will be helical, leading to a quantized spin Hall effect. More important, both QAH and QSH are expected to show a conductance of $4e^2/h$ in a

two-terminal transport experiment, in case the edge-states couple to the metallic contacts. However, as we have shown in a previous publication [22], this condition is not necessarily fulfilled in experiment, as the clean part of a sample that hosts the gapped phase can be separated from the metallic contacts by a more disordered phase. This disordered phase will not let edge-states penetrate to the contacts, but will confine them to isolated puddles in the sample center. For the LAF charge, spin and valley Hall conductances cancel out, no edge-states can form, and consequently LAF is expected to be fully insulating even in a two-terminal conductance measurement. Ignoring the effect of the magnetic field on the electron spins the LAF state has also been predicted to show a gap whose size is independent of a perpendicular magnetic field, whereas QAH and QSH should show a strong increase of the gap by 5.5 meV/tesla [20]. A theory including spin [26] however predicts the formation of a canted antiferromagnet (CAF) that shows a magnetic field dependence similar to that of QAH and QSH.

To identify the actual groundstate among the three candidates, it is useful to explore the three symmetries that might be preserved in them, namely time reversal symmetry \mathcal{T} , spin rotation symmetry (SU_2), and valley Ising symmetry (\mathcal{Z}_2) [20, 25]. In each of the three phases, only one symmetry is preserved: time-reversal symmetry \mathcal{T} in the QSH, spin rotational symmetry SU_2 in the QAH, and valley Ising symmetry \mathcal{Z}_2 for the LAF.

The valley Ising symmetry \mathcal{Z}_2 , a state being invariant under exchange of K and K', is broken in QAH and QSH, but is difficult to assess in a transport experiment. Time reversal symmetry \mathcal{T} is broken by the QAH and LAF, and the case of QAH would manifest in a spontaneous Hall conductance at zero magnetic field, and in general as an inequivalence of $G(B)$ and $G(-B)$. In a real world sample however, puddles of different sign of the Hall conductance would exist next to each other, so that a spontaneous Hall conductance would be unobservable. Spin rotation symmetry SU_2 , which is broken in the QSH and LAF, with the spins in the bottom and top layer being locked into an antiferromagnetic arrangement, can easily be assessed by looking at the response of the gap to a parallel magnetic field, to exclude any orbital effects that are responsible for the big response to perpendicular field. While LAF is a real antiferromagnet, with the spins in the top and bottom layer pointing into opposite directions, the QSH also has to be considered a phase with antiferromagnetic spin order, however with the spin orientation being opposite for different valleys. In both LAF and QSH, the electron spins are not free to move, and a response to parallel magnetic

field would be absent, as long as the Zeeman energy is smaller than the exchange interaction responsible for the antiferromagnetic spin arrangement [27]. In the QAH the electron spins are not ordered and would show a response to parallel field determined by the Zeeman splitting of the spin up and spin down levels. This would lead to a decrease of the gap Δ by $g\mu_B B$.

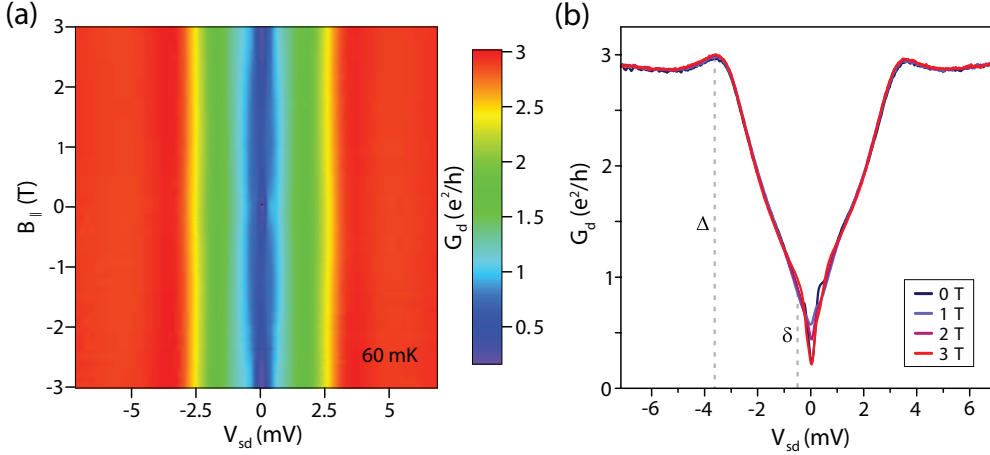


FIG. 4: a) G_d at the CNP as a function of parallel magnetic field B_{\parallel} and V_{sd} . b) Cuts through a) at several fixed magnetic fields.

In order to assess the response of Δ to a parallel magnetic field, we have performed nonlinear conductance measurements in a vector magnet system that allowed adjusting the orientation of the magnetic field vector with high precision. As the Zeeman splitting of the conduction electrons with $g=2$ is much smaller than the response of Δ to a perpendicular magnetic field, the proper adjustment of the direction of B_{\parallel} is crucial, and a small misalignment of a few degrees will lead to a perpendicular field component that will change Δ much more than what is expected from Zeeman splitting alone. Measurements were done with the sample mounted vertically, and B_{\parallel} was applied in the direction of the bilayer plane. As initial measurements showed an unreasonably large response of $G_d(V_{sd})$ to B_{\parallel} (see supplementary information), we checked the correct alignment of the sample plane by applying an additional, small magnetic field in the horizontal direction, maximizing the height of the BCS-like overshoot visible in $G_d(V_{sd})$ at $V_{sd} \approx 3.5$ meV (see figures 3b, 4b and supplementary information). We found that the sample had a slight misalignment of -1.6° with respect to the vertical direction, probably due to mechanical imperfections of the sample holder. Adding a small horizontal field component to the vertical magnetic field, we were

able to compensate for this misalignment and to adjust the magnetic field to the sample plane with a precision of 0.1° .

The results of a measurement of differential conductance at the CNP as a function of B_{\parallel} and V_{sd} are shown in figure 4. Compared to the conductance as a function of perpendicular field (figure 3) it is clear from figures 4a and 4b that the big gap Δ is not affected by a parallel magnetic field. Following the outer inflection points at $V_{sd} \approx 2.5$ mV we find a magnetic field dependence of less than $60 \mu\text{eV}/\text{tesla}$, which is significantly smaller than the electron spin Zeeman splitting of $116 \mu\text{eV}/\text{tesla}$ (see supplementary information for details). Our experimental results therefore allow us to exclude a change of Δ due to the Zeeman splitting of the conduction electrons. Note that a small dependence of G_d on B_{\parallel} occurs around zero bias $V_{sd} \approx 0$. We think however that this change in G_d does not originate from the clean phase in the sample center and is not related to the gap Δ . According to the previous paragraph, this result shows that the electronic phase that we have labeled Δ is a spin-ordered phase, where the electron spins are bound by some exchange interaction and do not respond to an external magnetic field. Looking at the spin properties of the three possible candidates for Δ , we can conclude that Δ is not the quantum anomalous Hall (QAH) state, but that it has to be one of the remaining two: the quantum spin Hall (QSH) or the layer antiferromagnet (LAF). To further distinguish QSH from LAF one could make use of the spin Hall effect in the QSH, which should lead to a finite spin accumulation on the Hall terminals of a Hall cross sample. Such a spin accumulation might be detectable via the inverse spin Hall effect, using a metal with strong spin-orbit scattering, such as palladium, as contact material on the Hall terminals. Due to the non optimal homogeneity of multi-terminal, current-annealed suspended graphene samples [22], the significance of such an experiment would however have to be evaluated very carefully.

In conclusion by performing nonlinear transport experiments on clean bilayer graphene for magnetic fields of perpendicular and parallel orientation we have shown that the groundstate at charge neutrality is gapped, and is a spin ordered phase. Of the three possible broken symmetry states that are suggested by theory, we can exclude that a quantum anomalous Hall state is realized in bilayer graphene. The groundstate has to be either the quantum spin Hall state, or the layer antiferromagnetic state. To distinguish the latter two from each other, further experimental work will be needed.

Acknowledgments

We acknowledge financial support by the Swiss NCCR on Nanoscience and Nanotechnology, the NCCR on Quantum Science and Technology, the ESF program Eurographene, the EU STREPS project SE2ND, and the Swiss National Science foundation.

-
- [1] K. S. Novoselov, A. K. Geim, S. V. Morozov, D. Jiang, Y. Zhang, S. V. Dubonos, I. V. Grigorieva, and A. A. Firsov, *Science* **306**, 666 (2004).
 - [2] M. I. Katsnelson, K. S. Novoselov, and A. K. Geim, *Nature Physics* **2**, 620 (2006).
 - [3] K. S. Novoselov, A. K. Geim, S. V. Morozov, D. Jiang, M. I. Katsnelson, I. V. Grigorieva, S. V. Dubonos, and A. A. Firsov, *Nature* **438**, 197 (2005).
 - [4] Y. Zhang, Y.-W. Tan, H. L. Stormer, and P. Kim, *Nature* **438**, 201 (2005).
 - [5] H. Min and A. H. MacDonald, *Phys. Rev. B* **77**, 155416 (2008).
 - [6] E. McCann and V. I. Fal'ko, *Phys. Rev. Lett.* **96**, 086805 (2006).
 - [7] H. Min, G. Borghi, M. Polini, and A. H. MacDonald, *Phys. Rev. B* **77**, 041407 (2008).
 - [8] Y. Barlas and K. Yang, *Phys. Rev. B* **80**, 161408 (2009).
 - [9] F. Zhang, H. Min, M. Polini, and A. H. MacDonald, *Phys. Rev. B* **81**, 041402 (2010).
 - [10] R. Nandkishore and L. Levitov, *Phys. Rev. Lett.* **104**, 156803 (2010).
 - [11] R. Nandkishore and L. Levitov, *Phys. Rev. B* **82**, 115124 (2010).
 - [12] O. Vafek and K. Yang, *Phys. Rev. B* **81**, 041401 (2010).
 - [13] Y. Lemonik, I. L. Aleiner, C. Toke, and V. I. Fal'ko, *Phys. Rev. B* **82**, 201408 (2010).
 - [14] Y. Barlas, R. Côté, K. Nomura, and A. H. MacDonald, *Phys. Rev. Lett.* **101**, 097601 (2008).
 - [15] J. Jung, F. Zhang, and A. H. MacDonald, *Phys. Rev. B* **83**, 115408 (2011).
 - [16] A. S. Mayorov, D. C. Elias, M. Mucha-Kruczynski, R. V. Gorbachev, T. Tudorovskiy, A. Zhukov, S. V. Morozov, M. I. Katsnelson, V. I. Falko, A. K. Geim, et al., *Science* **333**, 860 (2011).
 - [17] W. Bao, J. Velasco Jr., F. Zhang, L. Jing, B. Standley, D. Smirnov, M. Bockrath, A. H. MacDonald, and C. N. Lau, *PNAS* **109**, 10802 (2012).
 - [18] B. E. Feldman, J. Martin, and A. Yacoby, *Nature Phys.* **5**, 889 (2009).
 - [19] R. T. Weitz, M. T. Allen, B. E. Feldman, J. Martin, and A. Yacoby, *Science* **330**, 812 (2010).

- [20] J. Velasco, Jr., L. Jing, W. Bao, Y. Lee, P. Kratz, V. Aji, M. Bockrath, C. N. Lau, C. Varma, R. Stillwell, et al., *Nature Nanotech.* **7**, 156 (2012).
- [21] F. Freitag, J. Trbovic, M. Weiss, and C. Schönenberger, *Phys. Rev. Lett.* **108**, 076602 (2012).
- [22] F. Freitag, M. Weiss, R. Maurand, J. Trbovic, and C. Schönenberger, *Solid State Comm.* **152**, 2053 (2012).
- [23] H. J. van Elferen, A. Veligura, E. V. Kurganova, U. Zeitler, J. C. Maan, N. Tombros, I. J. Vera-Marun, and B. J. van Wees, *Phys. Rev. B* **85**, 115408 (2012).
- [24] A. Veligura, H. J. van Elferen, N. Tombros, J. C. Maan, U. Zeitler, and B. J. van Wees, *Phys. Rev. B* **85**, 155412 (2012).
- [25] F. Zhang, J. Jung, G. A. Fiete, Q. Niu, and A. H. MacDonald, *Phys. Rev. Lett.* **106**, 156801 (2011).
- [26] M. Kharitonov, *Phys. Rev. B* **86**, 195435 (2012).
- [27] F. Zhang and A. H. MacDonald, *Phys. Rev. Lett.* **108**, 186804 (2012).
- [28] Note that in our previous nomenclature[21, 22], the present sample falls into category B2a.

Spin Symmetry of the Bilayer Graphene Groundstate Supplementary Information

Frank Freitag, Markus Weiss,* Romain Maurand, Jelena Trbovic, and Christian Schönenberger
Department of Physics, University of Basel, Klingelbergstrasse 56, CH-4056 Basel, Switzerland
 (Dated: November 8, 2018)

I. SAMPLE ALIGNMENT PROCEDURE AND DATA AT FINITE ANGLE

As stated in the main text, the precise parallel alignment of the sample plane to the magnetic field was crucial. Measurements were done in a superconducting vector magnet system composed of a solenoid in z- and a split coil along the x-direction, as shown in figure 1. The sample was cooled down in dip-stick dilution refrigerator, that could

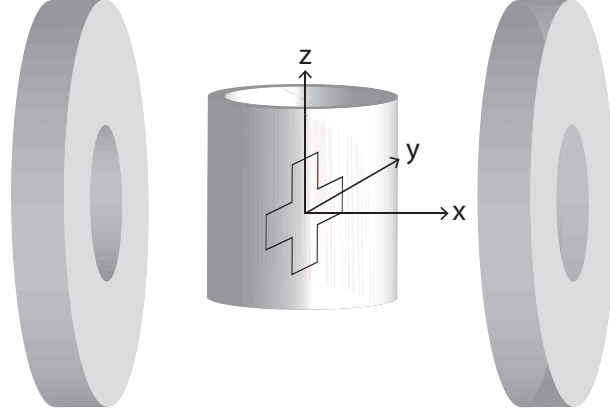


FIG. 1: Sketch of the vector magnet system and sample orientation.

be rotated around the z-axis. It was mounted vertically with the current contacts of the 4-terminal Hall cross roughly along the z-direction, and the Hall contacts roughly along the y-direction. The sample plane was aligned parallel to y-direction very precisely by applying a field of 1 tesla along the x-direction and rotating the dilution insert around the z-axis until the Hall signal was maximized. This was done at the charge neutrality point at elevated temperature ($T \approx 4.2\text{K}$), a parameter regime where the Hall resistance was linear in B_{\perp} . The result of initial measurements of $G_d(V_{sd}, B_z)$ done after this first alignment procedure are shown in figure 2.

As stated in the main text, we take the outer inflection points at $|V_{sd}| \approx 2.5\text{ mV}$ as a measure for the gap Δ .

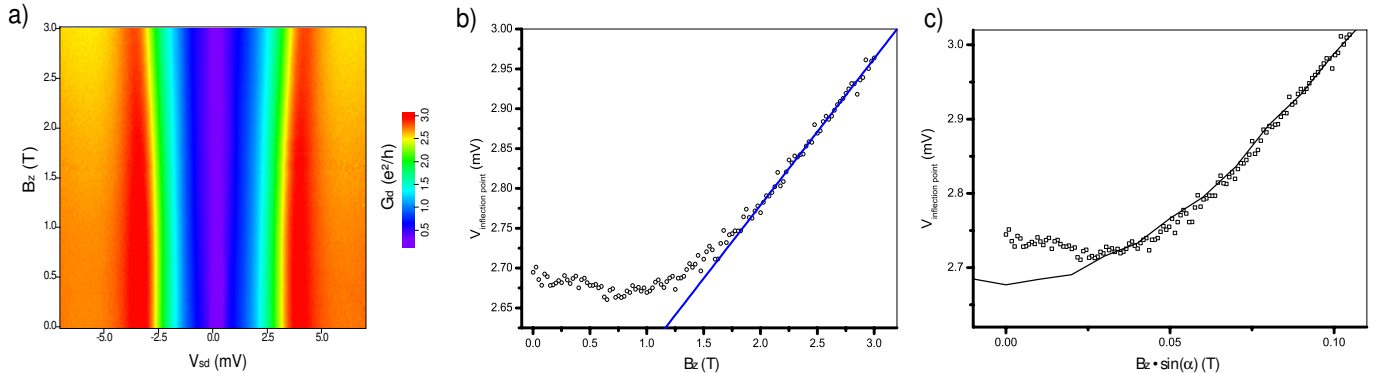


FIG. 2: a) Color scale plot of differential conductance as a function of source-drain voltage and B_z . b) Position of the inflection point as a function of B_z . The solid line is a linear fit for $2\text{T} \leq B_z \leq 3\text{T}$. c) The data from b) with the field axis rescaled by $\sin(\alpha)$, with $\alpha = 2.0^\circ$ (symbols). The solid line corresponds to the position of the first inflection point for perpendicular field orientation ($\alpha = 90^\circ$, see figure 3a in the main text).

Their position was determined by a numerical derivative of $G_d(V_{sd})$ and subsequent local fitting of the outer two

extrema with a gaussian. The average of the two inflection point positions at positive and negative bias voltage is shown in figure 2b. A linear fit for large B_z gives a magnetic field dependence of $183 \pm 4 \mu\text{V}/\text{T}$, significantly more than what is expected for Zeeman splitting ($116 \mu\text{V}/\text{T}$). This magnetic field dependence can be explained by the presence of a finite perpendicular field component that occurs due to a small tilt of the sample around the y-direction, probably due to mechanical imperfections of the sample holder. Rescaling the magnetic field axis by the sine of the effective angle between the sample plane and B_z , we can make the data coincide with the corresponding data for perpendicular magnetic field orientation, assuming a finite angle of $\alpha = 2.0^\circ$, as shown in figure 2c. The deviations visible for $B < 30 \text{ mT}$ might be due to some small nonlinearity in the x-axis magnet, that affected the measurement in perpendicular magnetic field.

To verify the misalignment angle, we applied a constant field of 1 tesla along the z-direction, and added a small field component along x, thereby slightly rotating the magnetic field vector around the y-axis. In order to find the perfectly parallel alignment of B we looked at the BCS-like peak in G_d at $V_{sd} \approx -3.4 \text{ mV}$ as a function of the small field component B_x applied in addition to $B_z = 1 \text{ T}$. Given previous investigations of the magnetic field dependence of Δ^1 (see also figure 3a in the main text), it is reasonable to assume that the peaks in $G_d(V_{sd})$ will be maximal for zero perpendicular field.

The results of such a measurement are shown in figure 3a. We found that G_d was maximized for $B_x = -28 \text{ mT}$ applied in addition to $B_z = 1 \text{ T}$, which corresponds to a rotation of the magnetic field vector of -1.6° around the y-axis. The difference to the value of 2.0° deduced from the scaling analysis in figure 2c could again be due to small nonlinearities in the x-axis magnet. Note also that this procedure allowed us to find the exact parallel field alignment quickly while keeping the sample at $T = 60 \text{ mK}$ and avoiding changes in G_d due to temperature drift caused by eddy current heating, that would be much more severe when sweeping the total magnetic field around zero. For all further measurements in parallel magnetic field B_z and B_x were driven synchronously in order to maintain the small tilt angle of -1.6° of the magnetic field vector.

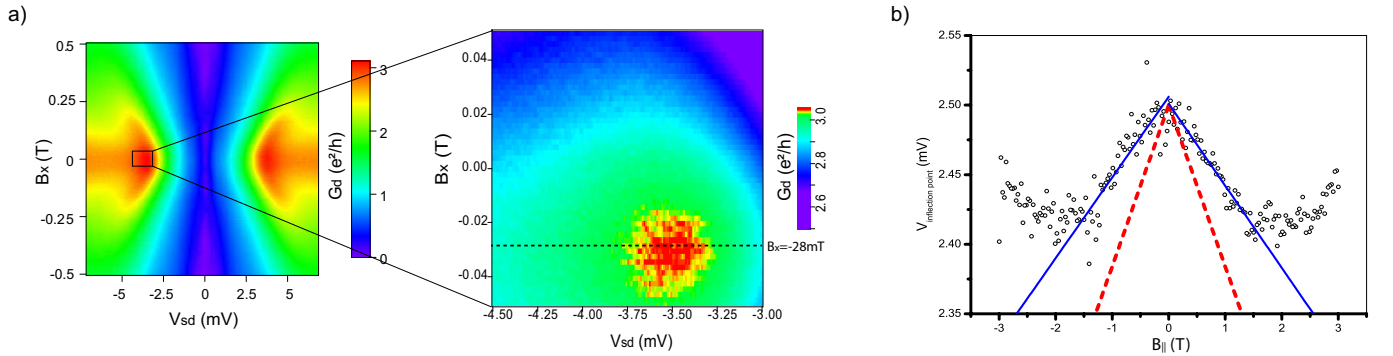


FIG. 3: a) $G_d(V_{sd}, B_x)$ measured close to the "BCS"-like peak at $V_{sd} \approx -3.5 \text{ mV}$ with a constant field B_z applied. The maximum of G_d occurs for $B_x = -28 \text{ mT}$. The left colorscale plot is figure 3a from the main text. b) Position of the inflection point extracted from the data shown in figure 4a of the main paper (symbols). The red dashed lines indicate the magnetic field dependence expected for Zeeman splitting of a spin with $g=2$ ($116 \mu\text{V}/\text{T}$). The blue solid lines are linear fits for $0 \leq B \leq 1.5 \text{ T}$, giving a magnetic field dependence of $61 \pm 2 \mu\text{V}/\text{T}$.

The data shown in figure 4a of the main text were measured this way, with no magnetic field dependence being visible to the naked eye. To do a more thorough check, we determined the position of the inflection points by numerical derivation and local fitting, as done for the data in figure 2. As can be seen in figure 3b, at small magnetic fields the inflection point shifts to lower voltages linearly with about $60 \mu\text{V}/\text{T}$, a tendency that changes drastically at larger magnetic fields. Although we currently do not know the reason for this non-monotonous behaviour, we can still exclude that this dispersion is due to Zeeman splitting of the conduction electrons, because in this case a much stronger shift of $116 \mu\text{V}/\text{T}$ would be expected.

II. TEMPERATURE DEPENDENCE

The temperature dependence of the equilibrium conductance $G(T)$ at the CNP is shown in figure 4. From 1.2 K down to base temperature the conductance decreases roughly by one order of magnitude, confirming the picture of a

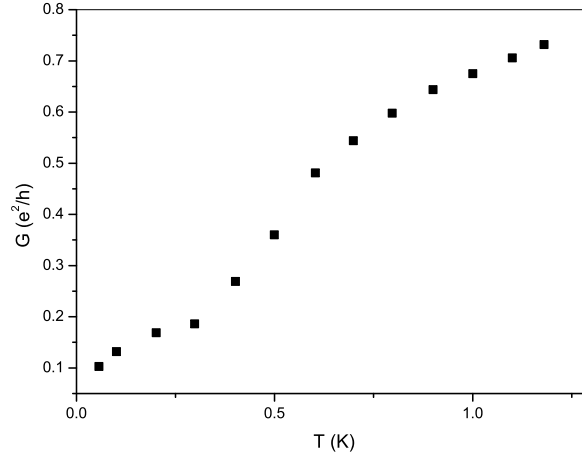


FIG. 4: Temperature dependence $G(T)$ at $B=0$ at the CNP.

gapped groundstate in bilayer graphene.

* Electronic address: Markus.Weiss@unibas.ch

¹ J. Velasco, Jr., L. Jing, W. Bao, Y. Lee, P. Kratz, V. Aji, M. Bockrath, C. N. Lau, C. Varma, R. Stillwell, et al., Nature Nanotech. **7**, 156 (2012).